TECHNICAL NOTES

NATIONAL ADVISORY COMMITTEE FOR AERONAUTICS

No. 528

WIND-TUNNEL TESTS OF A CYCLOGIRO ROTOR

By John B. Wheatley and Ray Windler
Langley Memorial Aeronautical Laboratory

Washington
May 1935

NATIONAL ADVISORY COMMITTEE FOR AERONAUTICS

TECHNICAL NOTE NO. 528

WIND-TUNNEL TESTS OF A CYCLOGIRO ROTOR

By John B. Wheatley and Ray Windler

SUMMARY

A cyclogiro rotor having a span and diameter of 8 feet was tested in the N.A.C.A. 20-foot wind tunnel. The tests showed that the cyclogiro would be able to ascend vertically, fly horizontally, and glide without power. The power required for normal flight would, however, be excessive. A comparison of calculated and experimental results showed that the analytical expressions used gave the correct variation of the power required with the rotor forces but that the values calculated for zero rotor forces were in error. It was also shown that the blade profile-drag coefficient was incorrectly assumed and that the error in the calculated power required arose from that assumption. The effect of oscillating an airfoil is considered a primary reason for the discrepancy between the assumed and experimental drag coefficients and research on an oscillating airfoil is believed to be necessary.

INTRODUCTION

During an extensive study of all types of rotating wings, the National Advisory Committee for Aeronautics examined the cyclogiro rotor and made an aerodynamic analysis of that system (reference 1). The examination disclosed that such a machine had sufficient promise to justify an experimental investigation; a model with a diameter and span of 8 feet was therefore constructed and tested in the 20-foot wind tunnel during 1934.

The experimental work included tests of the effect of the blade motion upon the rotor forces during the static-lift and forward-flight conditions at several rotor speeds and the determination of the relations between the forces generated by the rotor and the power required by it.

APPARATUS

The 20-foot wind tunnel, in which these tests were conducted, is described in reference 2; the only alteration required for the cyclogiro tests was the installation of two lateral-force balances. These balances were required because the rotor axis was mounted vertically and the resultant rotor force was measured on the drag and lateral-force balances.

The model cyclogiro rotor is shown ready for test in figure 1. Its essential dimensions are:

Span	8 ft.
Diameter	8 ft.
Number of blades	4
Blade chord	0.312 ft.

Each of the blades was attached to the rotor shaft by seven arms; ball-bearing pivots were provided in the blade at the 0.25-chord point and the blades were statically balanced about that point. The blade airfoil section was the N.A.C.A. 0012 modified so that the mean-camber line was an arc of 9-foot radius; the mean-camber line was chosen to coincide with the blade path during a representative condition of operation. The blade construction, shown in figure 2, was composite, consisting of a continuous spar, a nosepiece containing a lead balance weight, wooden ribs, a metal trailing edge, and a covering of silk paper. Every effort was made to save weight without sacrificing strength but because the filler blocks between spar and ribs were too small two blades were broken in a preliminary test when the ribs pulled away from the spar. No further trouble was experienced after the weak joint had been strengthened by larger filler blocks.

The blade angle, measured from a tangent to the blade circle, was controlled by link rods that connected the trailing edge of the blades at their lower ends to the outer race of an eccentric ball bearing on the rotor axis. The eccentricity, which determined by its magnitude and direction the amplitude and phase of the blade oscillation, was the resultant of two circular eccentrics that could be rotated both with respect to the rotor axis and to each

other; this arrangement obviously makes possible the development of an eccentricity of any desired magnitude below the maximum in any direction. The amplitude of the maximum blade angle was limited by the geometry of the model to about 35°.

PROCEDURE AND TESTS

A considerable amount of work was necessary to attain satisfactory balance on the model. The cantilever rotor proved to be extremely sensitive to an unbalance of a few inch-ounces so that practically perfect static balance was required before the balance scales were sufficiently steady to permit the taking of accurate readings. It was also found necessary to stiffen the shaft to raise its critical speed above the operating speed.

During preliminary tests the model was examined with a stroboscope to determine qualitatively the lag of the eccentric bearing race behind the blades and the twist of the blades. The examination disclosed little except that these quantities were too small to be detected.

The procedure during test consisted of setting the amplitude and phase angle of the rotor eccentricity to predetermined values at a given tunnel speed and rotor speed and taking simultaneous visual observations of the dynamic pressure and the six balance scale readings.

Tare tests.- Complete tare runs were made with the blades removed from the rotor. This procedure did not determine the interference effects on the blades of the blade-supporting arms but supplied a reasonably accurate approximation of the forces on the parasitic rotor structure. The test results in this paper were obtained by subtracting from the gross forces on the rotor the forces obtained with the blades removed.

Static lift.- Force measurements on the model were made at several rotor tip speeds with the wind tunnel stopped. The major rotor force was developed along the tunnel axis and resulted in an induced flow in the tunnel; the flow was slight, however, and was ignored with very small resultant error. An additional test was made at constant tip speed and eccentricity in which the phase angle was changed successively by 30° steps. The influence on the rotor of the fluid boundaries was indicated by an

increase of 7 percent in the magnitude of the force developed when its direction was changed from along the tunnel axis to across the tunnel axis.

Forward flight.- Force measurements were made at several rotor tip speeds and through a wide range of air speeds for the forward-flight tests. Level flight was simulated in that the resultant force was approximately perpendicular to the tunnel axis. A wide range of eccentricity amplitudes and phases was used, so that the characteristics of flight with and without power could be determined.

RESULTS

The results are presented in coefficient form, using the notation given in reference 1; for convenience, the coefficients are defined below.

$$C_X = \frac{X}{\rho \Omega^2 R^3 s} \quad (1)$$

$$C_Z = \frac{Z}{\rho \Omega^2 R^3 s} \quad (2)$$

$$C_P = \frac{P}{\rho \Omega^3 R^4 s} \quad (3)$$

$$\mu = \frac{V \cos \theta}{\Omega R} \quad (4)$$

where X is the horizontal component of resultant rotor force, lb.

Z, vertical component of resultant rotor force, lb.

ρ, air density, slug/cu.ft.

Ω, rotor angular velocity, rad./sec.

R, rotor radius, ft.

V, air speed, ft./sec.

s, rotor span, ft.

P, power required, ft.-lb./sec.

θ, flight-path angle, deg. (measured from horizontal).

C_X, coefficient of horizontal rotor force.

C_Z, coefficient of vertical rotor force.

C_P, coefficient of power required.

μ, tip-speed ratio.

Forces in the Z direction (normally upward) are positive toward the side of the rotor where the blade is traveling with the relative wind; forces in the X direction (normally forward) are positive toward the side of the rotor where the blade is moving toward the positive Z axis. The eccentricity is defined by the amplitude α_A and phase angle ϵ of the forced oscillation of the blades. The blade angle is measured from the tangent to the blade circle; and phase angle is measured in the direction of rotation from horizontally upstream to the point at which the blade reaches its maximum angle. The use of the terms "horizontal" and "vertical" should be understood to apply to the rotor in its normal position with the axis horizontal. All results as presented apply approximately to blades alone, the tare obtained from runs with blades removed having been subtracted from the gross results, as previously noted.

The data obtained for static lift are shown in figures 3 to 6. C_Z, C_X, and C_P are shown in figures 3 to 5 as functions of α_A for tip speeds of 74.5 ft./sec., 96.5 ft./sec., and 150 ft./sec.; figure 6 contains the same data in the form of polar curves of C_Z as a function of C_P.

Data for the forward-flight condition are presented in figures 7 to 13 for a tip speed of 150 ft./sec. Each figure contains data for a given tip-speed ratio from 0.20 to 0.50. The figures contain plots of C_Z against C_P for different constant values of C_X and a parametric plot of α_A and ϵ against C_P and C_Z.

The figures may be used as follows: The required values of C_Z and C_X determine the value of C_P on one plot; then the consequent values of C_Z and C_P determine the required values of α_A and ϵ on the other plot.

The results obtained at a tip speed of 96.5 ft./sec. are compared with those obtained at 150 ft./sec. in figure 14, where C_P is plotted against C_Z for several values of C_X at a tip-speed ratio of 0.50.

A comparison between computed and experimental results is presented graphically in figures 15 to 17. The power required to overcome the blade profile drag and the values of the blade profile-drag coefficient are shown in figure 15 for C_Z and $C_X = 0$; the variation of C_P with C_Z for $C_X = 0$ is shown in figure 16 and C_P as a function of C_X for $C_Z = 0$ is shown in figure 17. Figures 16 and 17 represent conditions for a tip-speed ratio of 0.50.

ACCURACY

Balance forces were read to ±0.1 lb. and, since the torque arm was 6 feet, the torque was obtained to ±0.6 lb.-ft. No corrections have been made in the results for jet-boundary or blocking effect because quantitative values for this lifting system were so uncertain; as a result, measured drag or X forces are thought to be slightly too high. The values from the faired curves of the coefficients are considered to be accurate within the following limits:

C_Z ±0.0005

C_X $\begin{matrix} 0.0008 \\ -0.0002 \end{matrix}$

C_P ±0.0005

CYCLOGIRO PERFORMANCE

The test results are here utilized in the calculation of the performance of a machine employing two rotors sim-

ilar in form to the one tested. The constants of the machine are:

Rotor loading $\frac{W}{2Rs}$ $= 5.0$ lb./sq.ft.

Rotor lift coefficient C_Z $= 0.05$

Parasite drag D_P $= \frac{W}{250} q$

Rotor thrust coefficient C_X $= \frac{D_P}{\rho \Omega^2 R^2 s} = 0.02 \mu^2$

Rotor tip speed $\Omega R = \left(\frac{W}{C_Z \rho R s}\right)^{\frac{1}{2}} = 290$ ft./sec.

Parasite torque, added power required coefficient $C_{P_T} = 0.0012 (1 + \mu^2)$

It is assumed that the actual machine will have a parasite rotor torque considerably less than the model. The results for the model indicated that the tare power requirement of the rotor was very closely expressed as $C_{P_T} = 0.0040 (1 + \mu^2)$ and, because the parasite structure was oversize and not of good streamline shape, it is estimated that this could be reduced to approximately 30 percent of the model value at full scale. The results of this calculation are shown in figure 18, together with the results based upon an average blade profile-drag coefficient of 0.015 for comparison.

The autorotational characteristics of the cyclogiro are presented in figure 19; the calculations are based on the experimental results and on the same constants and assumptions that were used for the results shown in figure 18. As in figure 18, autorotation has also been computed for $C_{D_o} = 0.015$. The equations of equilibrium have been applied to the test results to determine at what flight-path angle the weight and parasite drag are canceled by the rotor with zero resultant power coefficient; these equations result in the following expressions:

$$W \cos \theta = Z$$

$$Z \sin \theta = (X - D_p) \cos \theta$$

$$P = -P_T$$

Consequently,

$$C_Z = 0.05 \cos \theta$$

$$\sin \theta = \frac{C_X - 0.02 \mu^2}{0.05}$$

$$C_P = -C_{P_T}$$

DISCUSSION

Lag of the blade motion and blade twist would mean that the effective amplitude and phase of the blade motion were not identical with those of the eccentric but would not change the fundamental relationships between C_X, C_Z, and C_P. The fact that they were too small to be detected is sufficient reason to consider them unimportant, although the experimental values of α_A and ϵ are not considered exact.

Tare.- The test results presented in graphic form represent the differences between the tests of the complete rotor and the same rotor with the blades removed. The parasitic structure of the model rotor is not a scale equivalent of an actual flying rotor. In addition, the drag coefficient of a unit length of the model blade arms was found, from the tare results, to be 0.10 (based on the chord), which is quite large compared to a good strut section. It is thought that the forces on the parasite structure of another rotor can be calculated with little difficulty. Rather than undertake the difficult problem of deciding upon the ideal dimensions and form of a full-scale rotor supporting structure and calculating its drag and required power, the forces for the blades alone are presented and can thus be added to the calculated forces for the supports of another rotor.

Static lift.- It will be seen in figures 3 to 5 that C_X was not zero during the static-lift tests despite the fact that the phase angle was set to give such a result. The resultant force was inclined about 10° from the desired direction when α_A was 20°, a shift that is greater than any possible lag between the blade motion and the eccentric. The lateral component of the resultant may be

qualitatively explained as a Magnus effect upon the rotor shaft because the rotor force would generate an induced velocity of appreciable magnitude in the interior of the rotor. Although the magnitude of the actual Magnus effect on the shaft cannot be accurately estimated, an approximate calculation disclosed that it would be at least a third of the observed lateral force.

The results of the tests at different tip speeds show reasonable agreement and indicate that the scale effect is small over the range tested. The lift per horsepower can be calculated from these curves by means of the expression

$$L/hp. = \frac{550\ C_Z}{\Omega R\ C_P}$$

which follows from the definition of the coefficients. For a tip speed of 100 feet per second, the maximum lift per horsepower is about 23.8 lb./hp. The same quantity for an airplane propeller set to 10° pitch and operating at 100 feet per second tip speed is about 50 lb./hp. (reference 3).

Forward flight.- Figures 7 to 13 show that the power required for the rotor increases much faster with C_X than with C_Z; also, that to a first approximation, the curves of constant C_X are mutually parallel. It is evident from the curves that C_Z is primarily a function of ϵ and not of α_A and that C_P changes very slowly with ϵ and rapidly with α_A; since C_P varies rapidly with C_X, it follows that to a first approximation, α_A determines C_X and C_P, and ϵ fixes the value of C_Z. This result is predicted from the equations developed in reference 1.

Performance.- The interpretation of the test results obtained by applying them to the calculation of the performance of a machine employing this lifting system as shown in figure 18 is not encouraging. Vertical ascent is possible only with a power of 0.15 hp./lb.; inversely, a power loading of 6.67 lb./hp. would be necessary. With this power loading, a maximum speed of about 106 miles per hour and a maximum rate of climb at 50 miles per hour of about 2,400 ft./min. would be obtained. With a normal power loading of 10 lb./hp., however, the speed range is from 29 to 77 miles per hour and the maximum rate of

climb at 50 miles per hour is 790 ft./min. The constants determining the performance have been chosen on the favorable side; consequently, the performance shown in figure 18 is considered optimistic.

The autorotational performance plotted in figure 19 has not shown the velocity in vertical descent because the experimental results did not include this condition. The gliding performance is, in general, poor. The minimum vertical velocity is approximately 20 miles per hour and increases rapidly as the horizontal speed becomes less than 40 miles per hour. The minimum gliding angle is about -25°.

Comparison of analysis and experiment.- Figure 15 shows that the value of the average blade profile-drag coefficient C_{D_o} is, in reality, a function of tip-speed ratio and is not constant as was assumed; the experimental C_{D_o} rises to the unexpected value of 0.04 at a tip-speed ratio of 0.50. Consequently, the calculated power for zero rotor force is much too small. The increase in drag coefficient is similar to the increase that was observed by Katzmayr (reference 4) when he measured the average drag of an airfoil oscillating in a steady air stream. It should be noted that the results in figure 15, although for zero rotor forces, nevertheless correspond to an oscillation in angle of attack over a range greater than $\pm 10^{\circ}$. There exists a real possibility, substantiated by these and by Katzmayr's tests, that an oscillating airfoil has characteristics that are entirely unlike those of a stationary airfoil, and research on the oscillating airfoil is of fundamental importance in the whole field of rotating-wing research. Many questions now unanswered will become clear when the laws which govern the oscillating airfoil are understood.

Figures 16 and 17 show that the equations in reference 1 would give close agreement with the experimental results if the value of C_{D_o} were correctly chosen; the calculated curves of C_Z and C_X as functions of C_P are parallel to the experimental values but intersect the ordinate axis at too small a value. This result is considered a reasonable verification of the mathematical analysis.

CONCLUSIONS

1. The cyclogiro is capable of vertical ascent, forward flight, and gliding flight without power.

2. The probable performance of the cyclogiro is very poor for normal power loadings, and a maximum speed of 100 miles per hour would be attained only with a power loading of less than 7 lb./hp.

3. The variation of the power required by the cyclogiro with the vertical and horizontal force coefficients is correctly predicted by mathematical analysis.

4. The profile-drag coefficient of the cyclogiro rotor blades increases rapidly with tip-speed ratio and is probably influenced by the blade oscillations.

5. Research on the oscillating airfoil is needed in order to clarify past and future rotating-wing research.

Langley Memorial Aeronautical Laboratory,
National Advisory Committee for Aeronautics,
Langley Field, Va., February 26, 1935.

REFERENCES

1. Wheatley, John B.: Simplified Aerodynamic Analysis of the Cyclogiro Rotating-Wing System. T.N. No. 467, N.A.C.A., 1933.

2. Weick, Fred E., and Wood, Donald H.: The Twenty-Foot Propeller Research Tunnel of the National Advisory Committee for Aeronautics. T.R. No. 300, N.A.C.A., 1928.

3. Diehl, Walter S.: Ststic Thrust of Airplane Propellers. T.R. No. 447, N.A.C.A., 1932.

4. Katzmayr, R.: Effect of Periodic Changes of Angle of Attack on Behavior of Airfoils. T.M. No. 147, N.A.C.A., 1922.

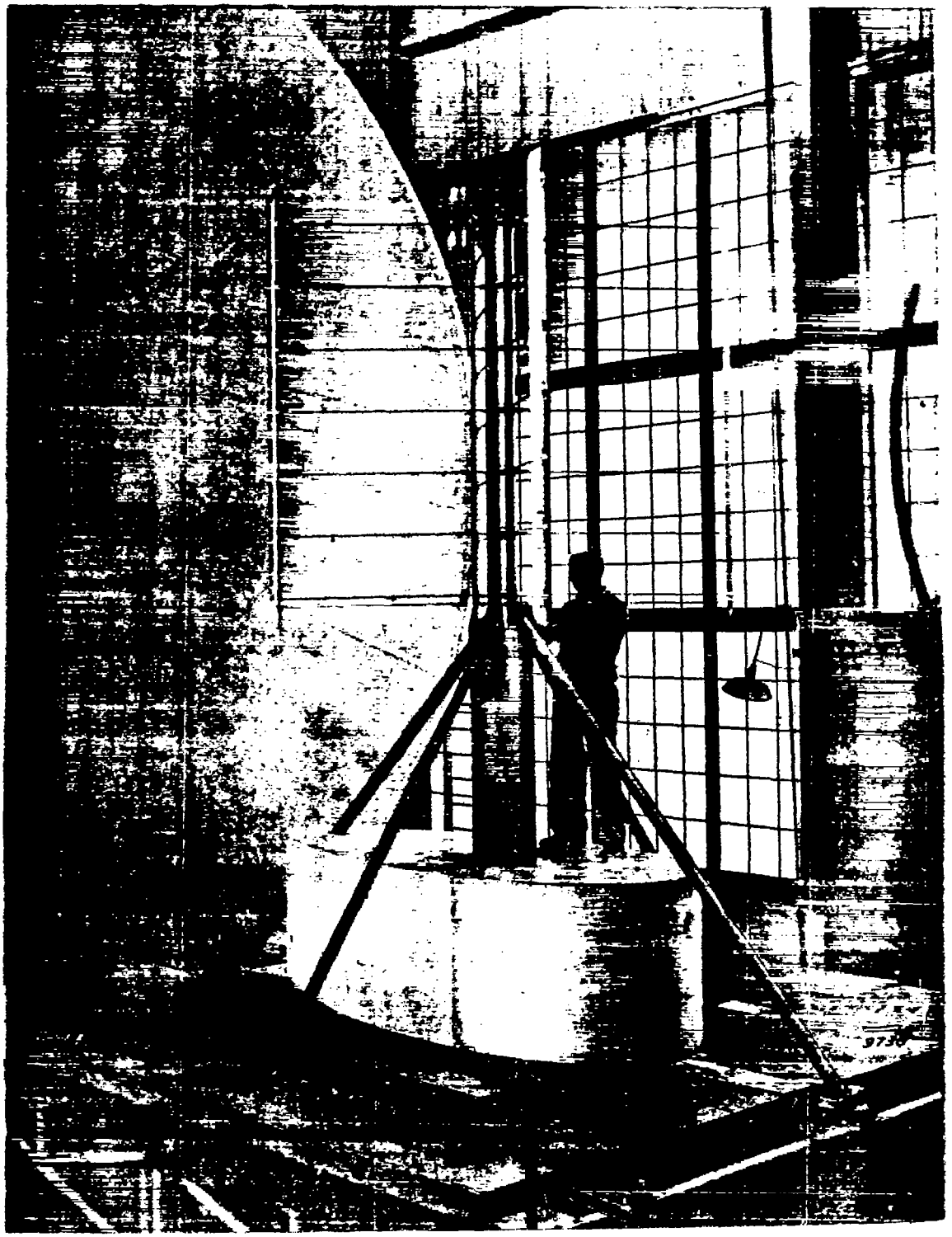

Figure 1.-The cyclogiro rotor set up for testing.

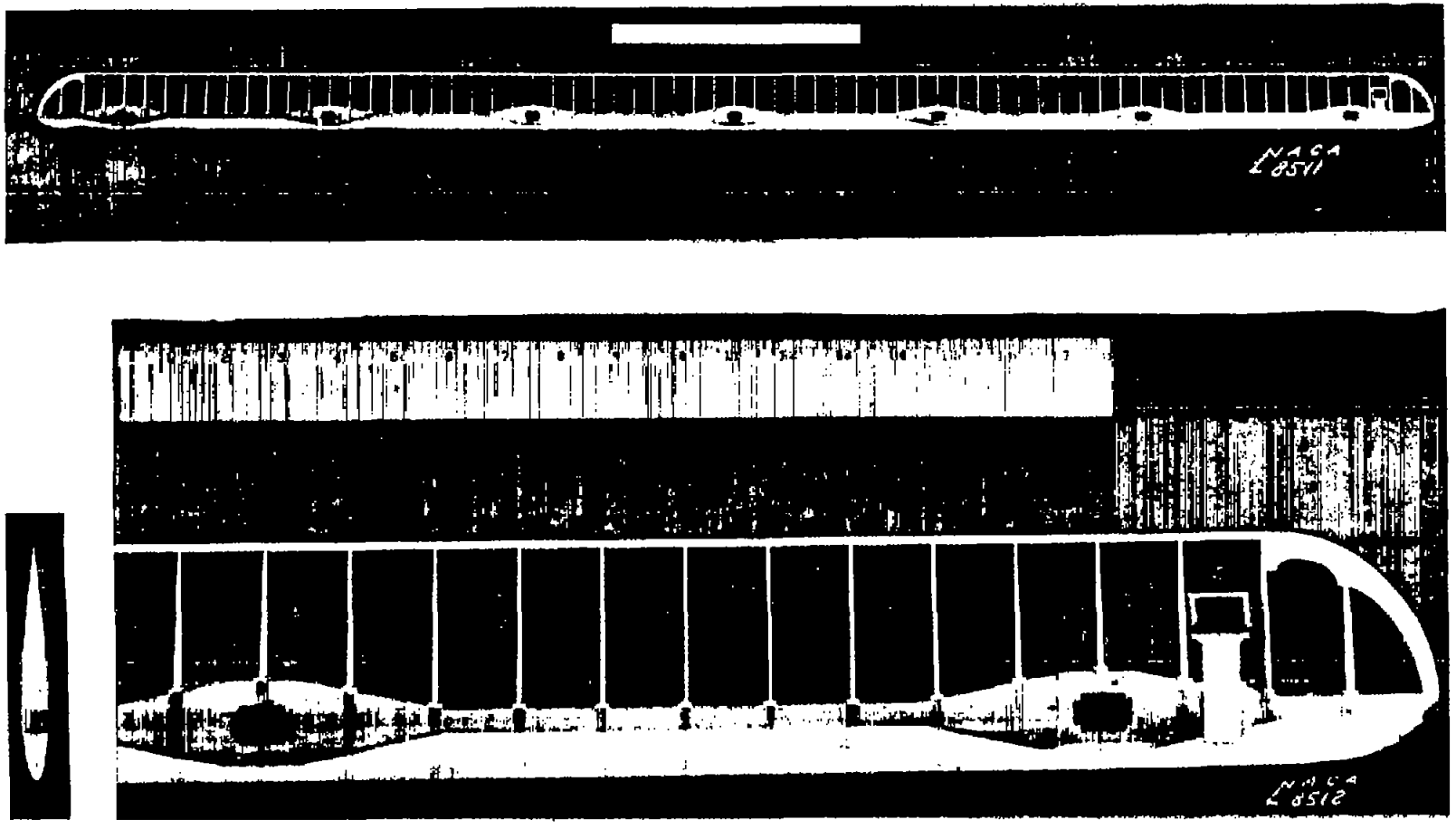

Figure 2.-Details of the cyclogiro blade.

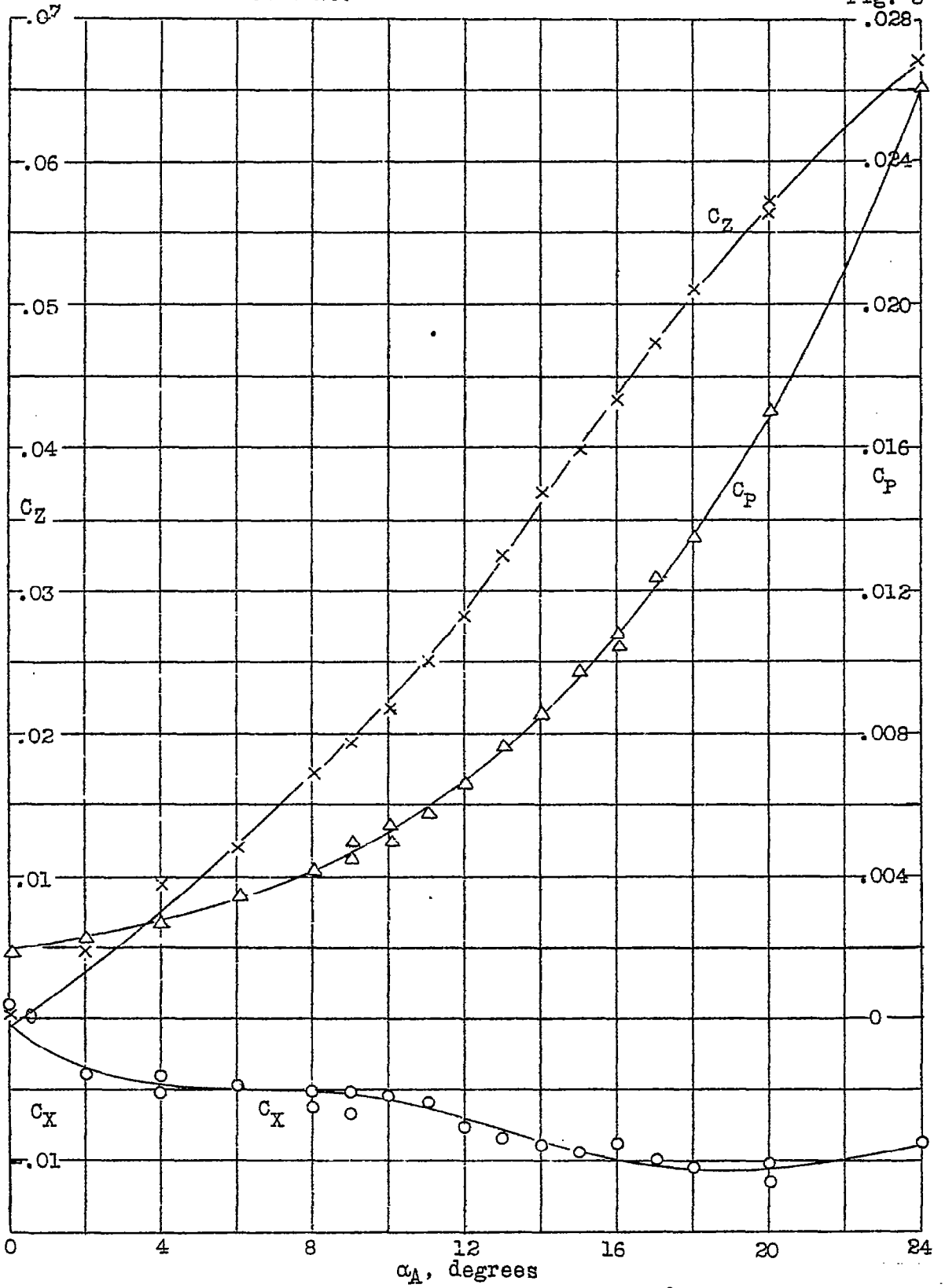

Figure 3.-Static lift. Blades alone; $\epsilon = 0^\circ$; $\Omega R = 74.5$

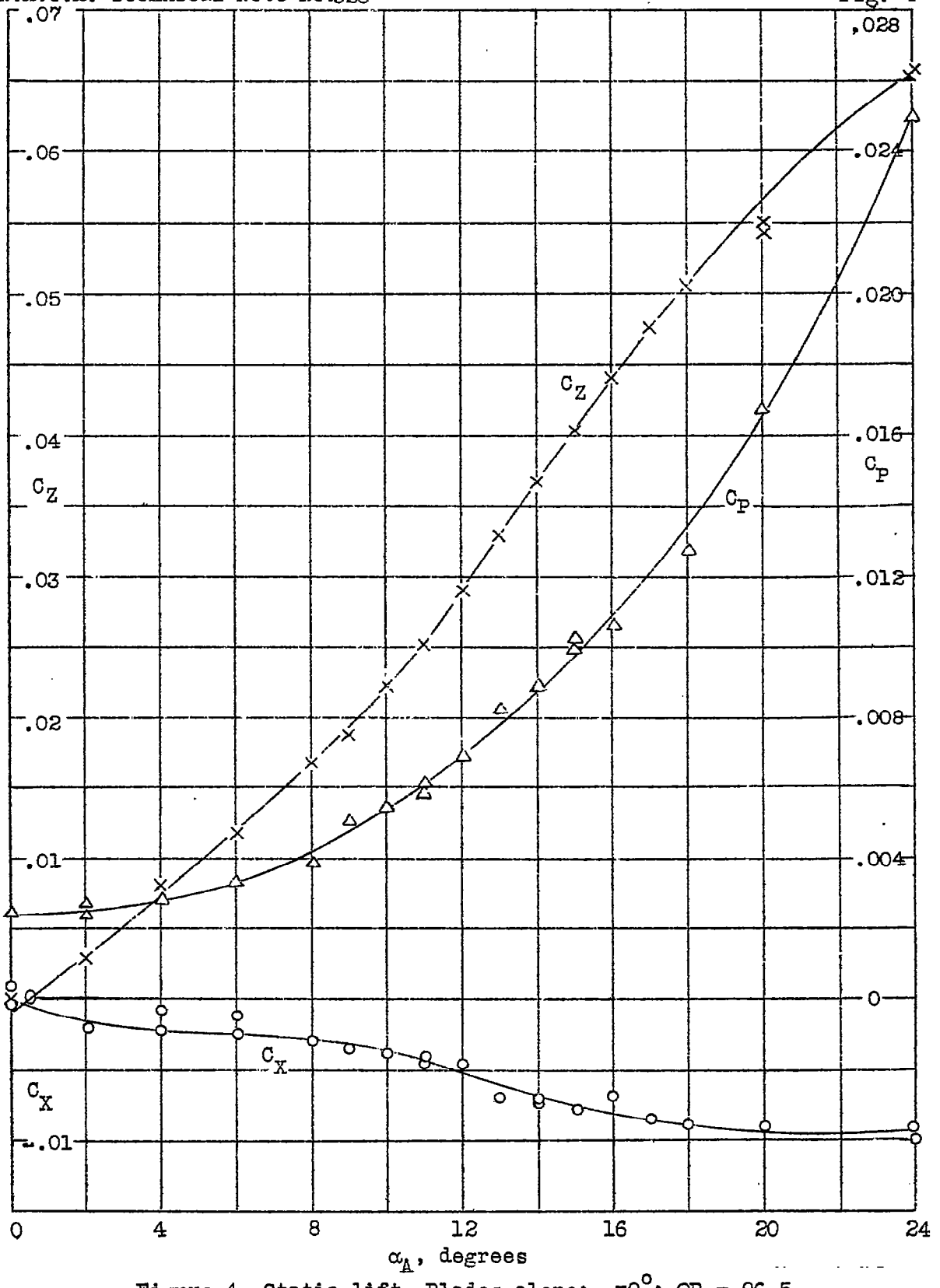

Figure 4.-Static lift. Blades alone; $\epsilon=0^{\circ}$; $\Omega R = 96.5$

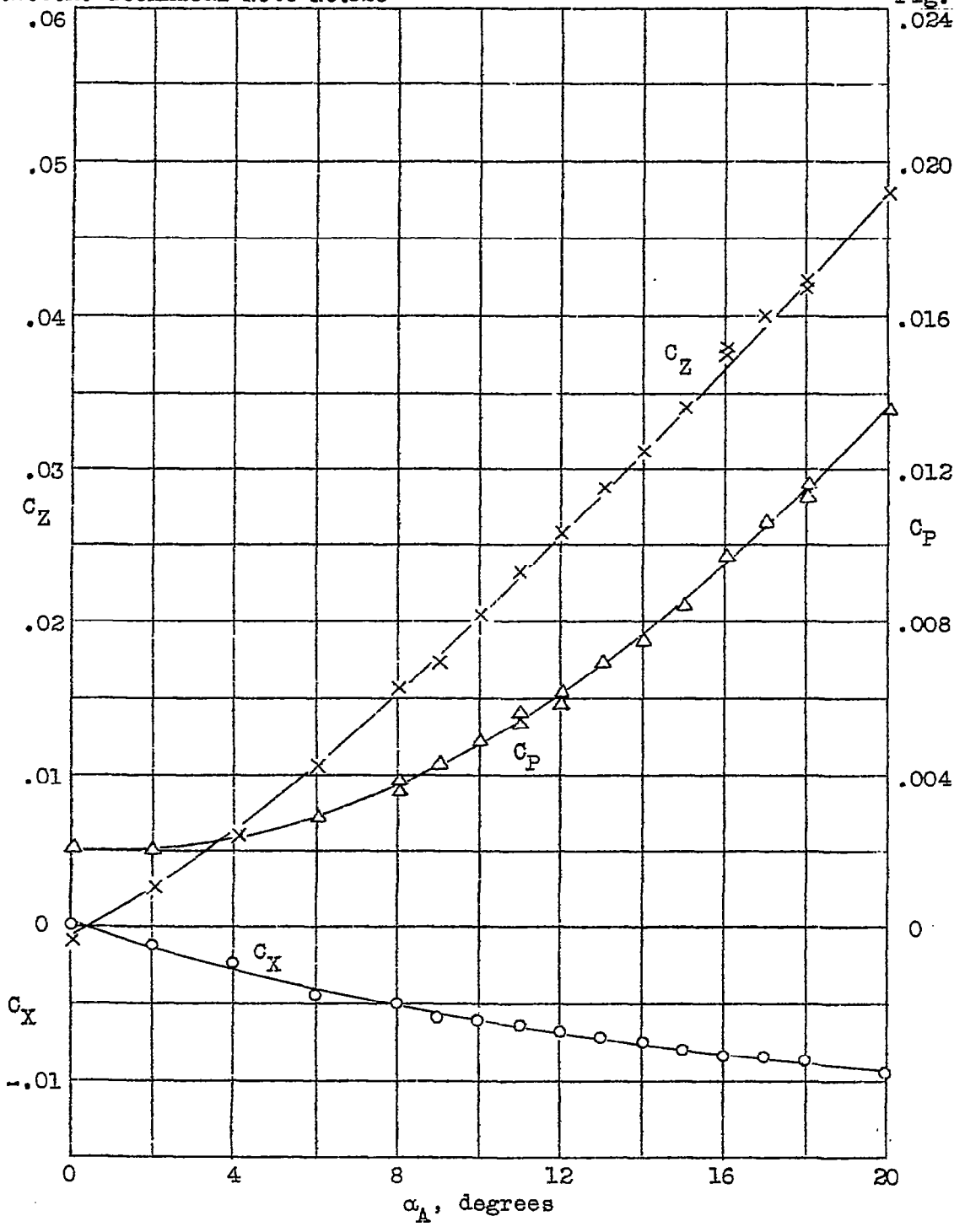

Figure 5.-Static lift. Blades alone; $\epsilon = 0^\circ$; $\Omega R = 150$

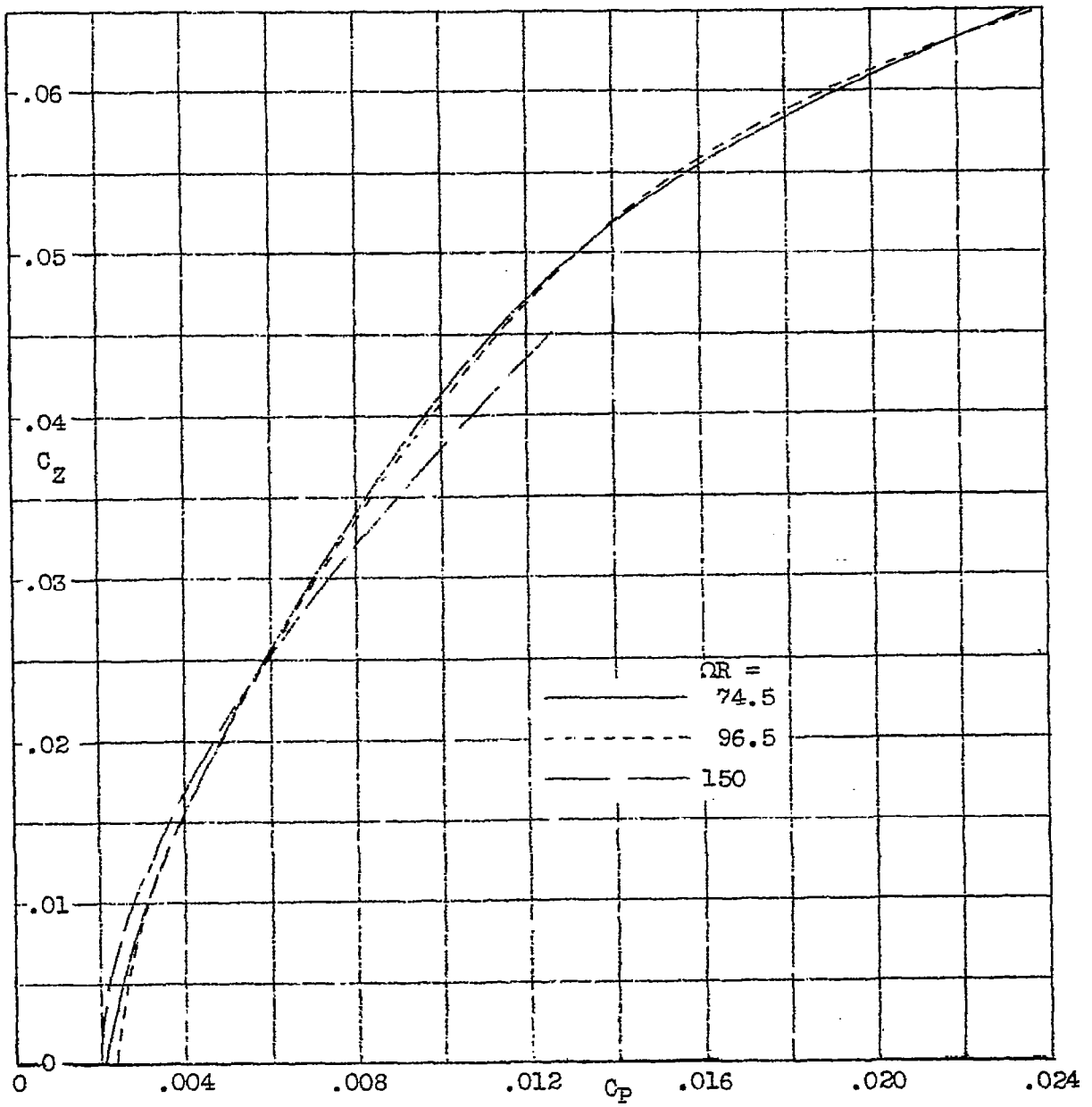

Figure 6.-Power polar. Static lift. Blades alone; $\epsilon = 0^\circ$.

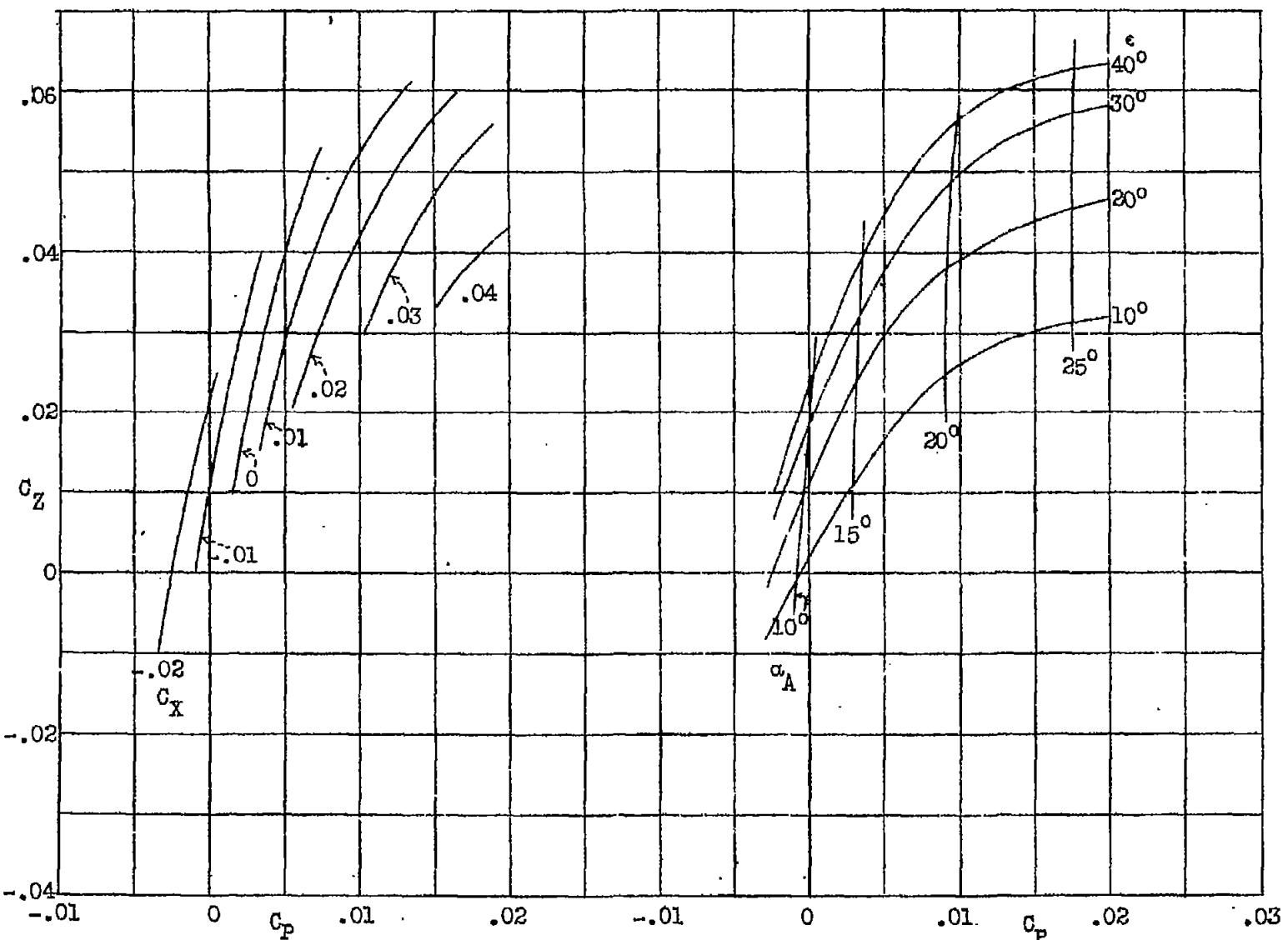

Figure 7.-Level flight. Blades alone; $\Omega R = 150$; $\frac{V}{\Omega R} = 0.20$

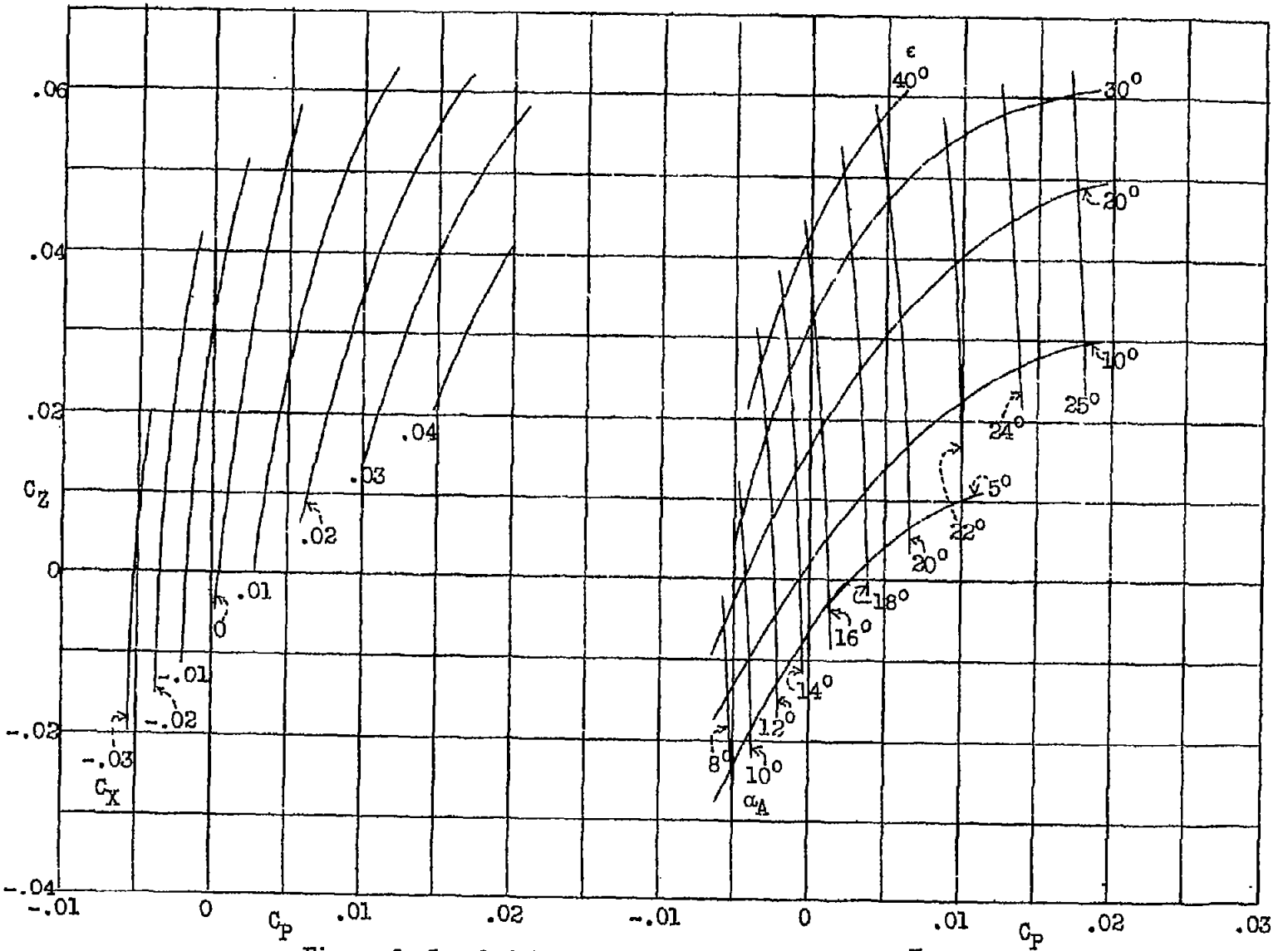

Figure 8.-Level flight. Blades alone; $\Omega R = 150$; $\frac{V}{\Omega R} = 0.25$

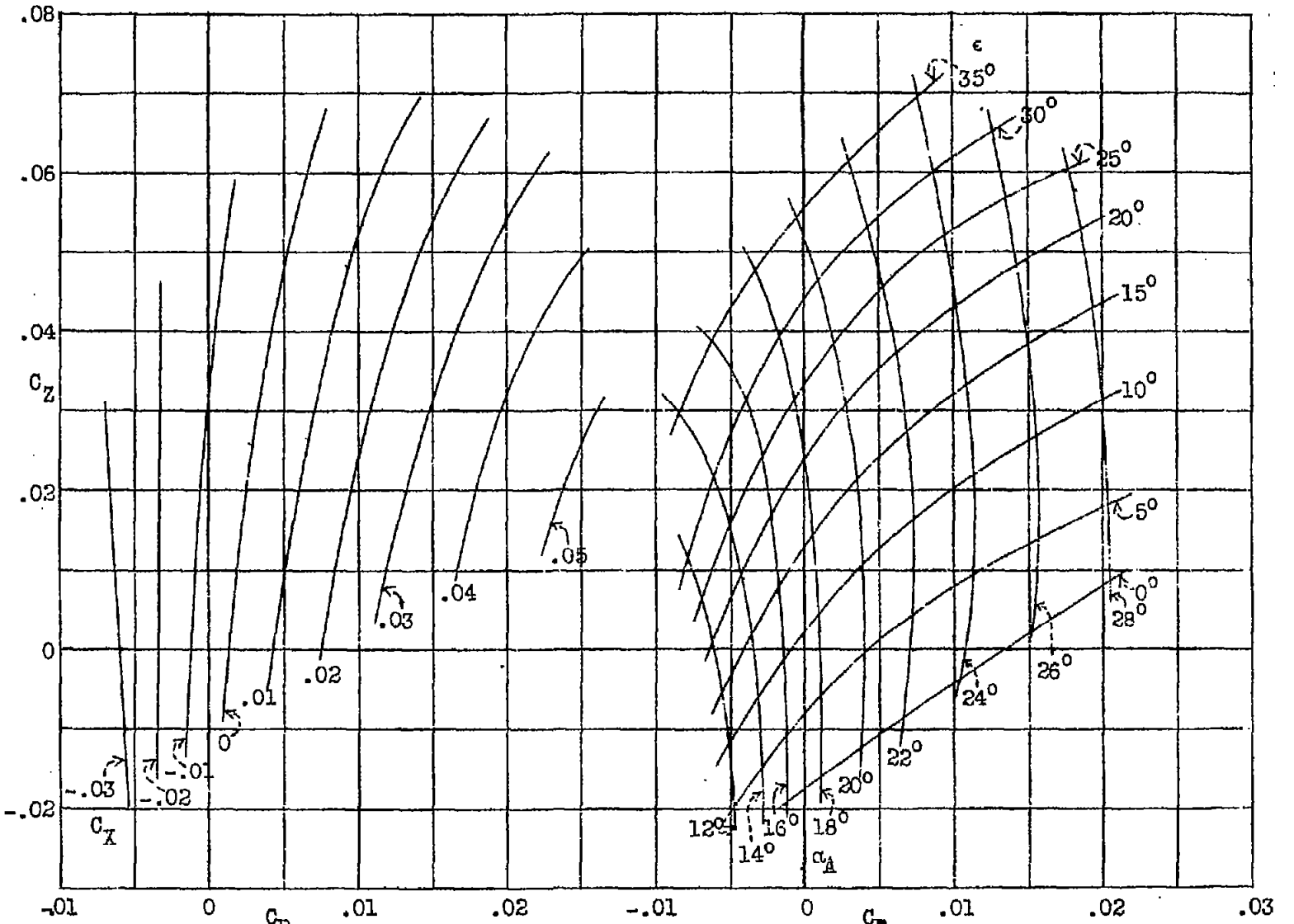

Figure 9.-Level flight. Blades alone; $\Omega R = 150$; $\frac{V}{\Omega R} = 0.30$

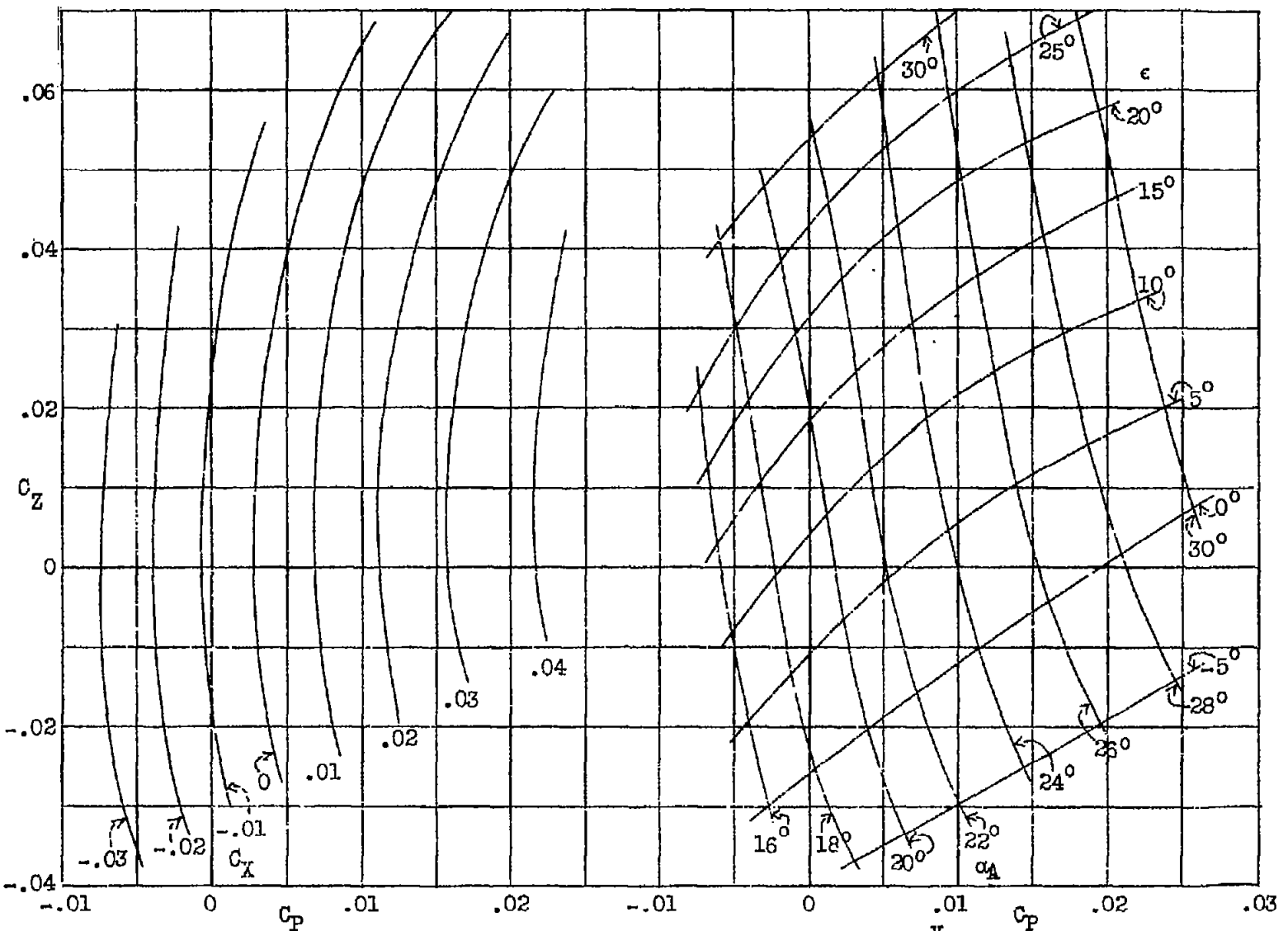

Figure 10.-Level flight. Blades alone; $\Omega R = 150$; $\frac{V}{\Omega R} = 0.35$

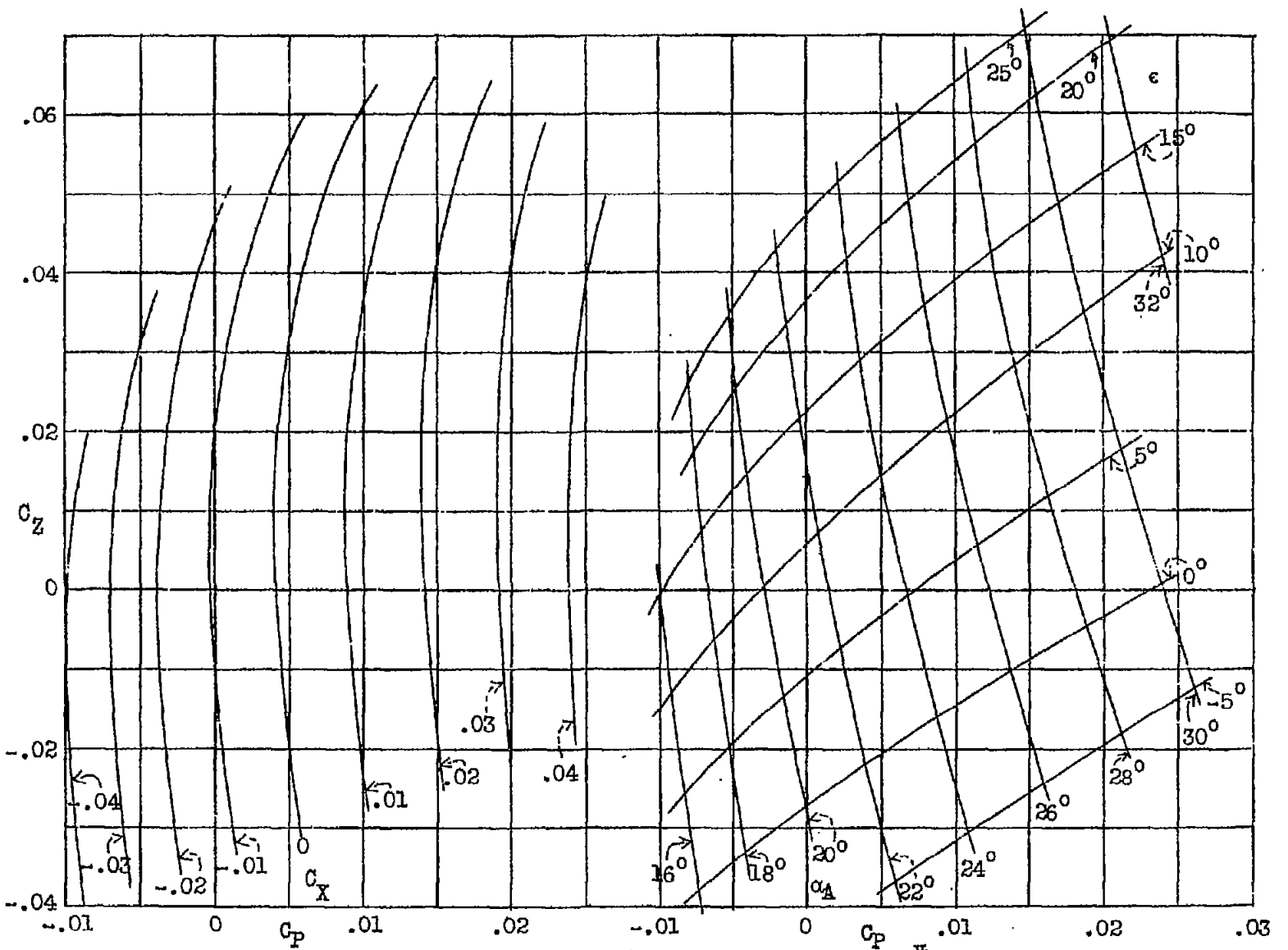

Figure 11.-Level flight. Blades alone; $\Omega R = 150$; $\frac{V}{\Omega R} = 0.40$

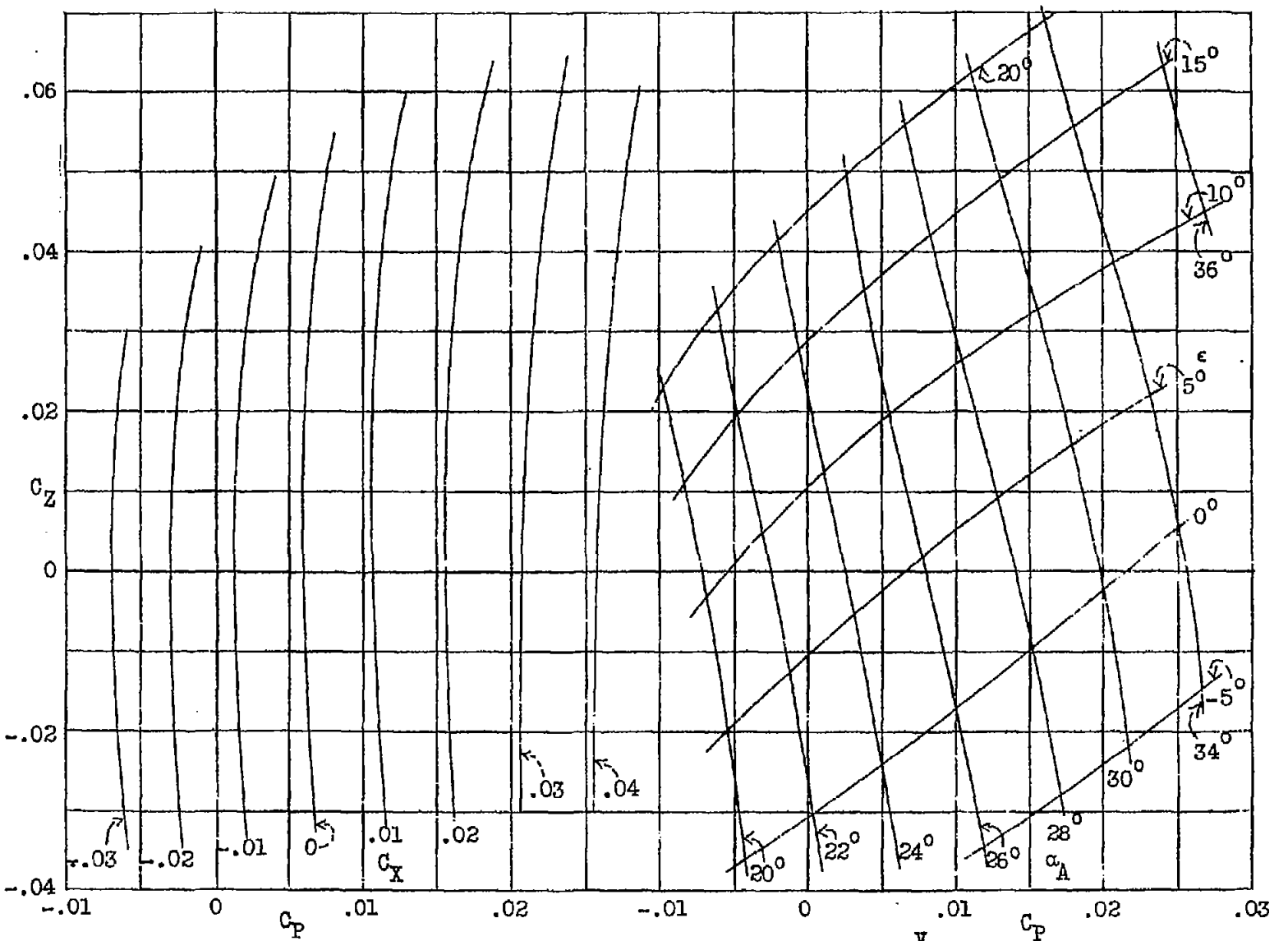

Figure 12.-Level flight. Blades alone; $\Omega R = 150$; $\frac{V}{\Omega R} = 0.45$

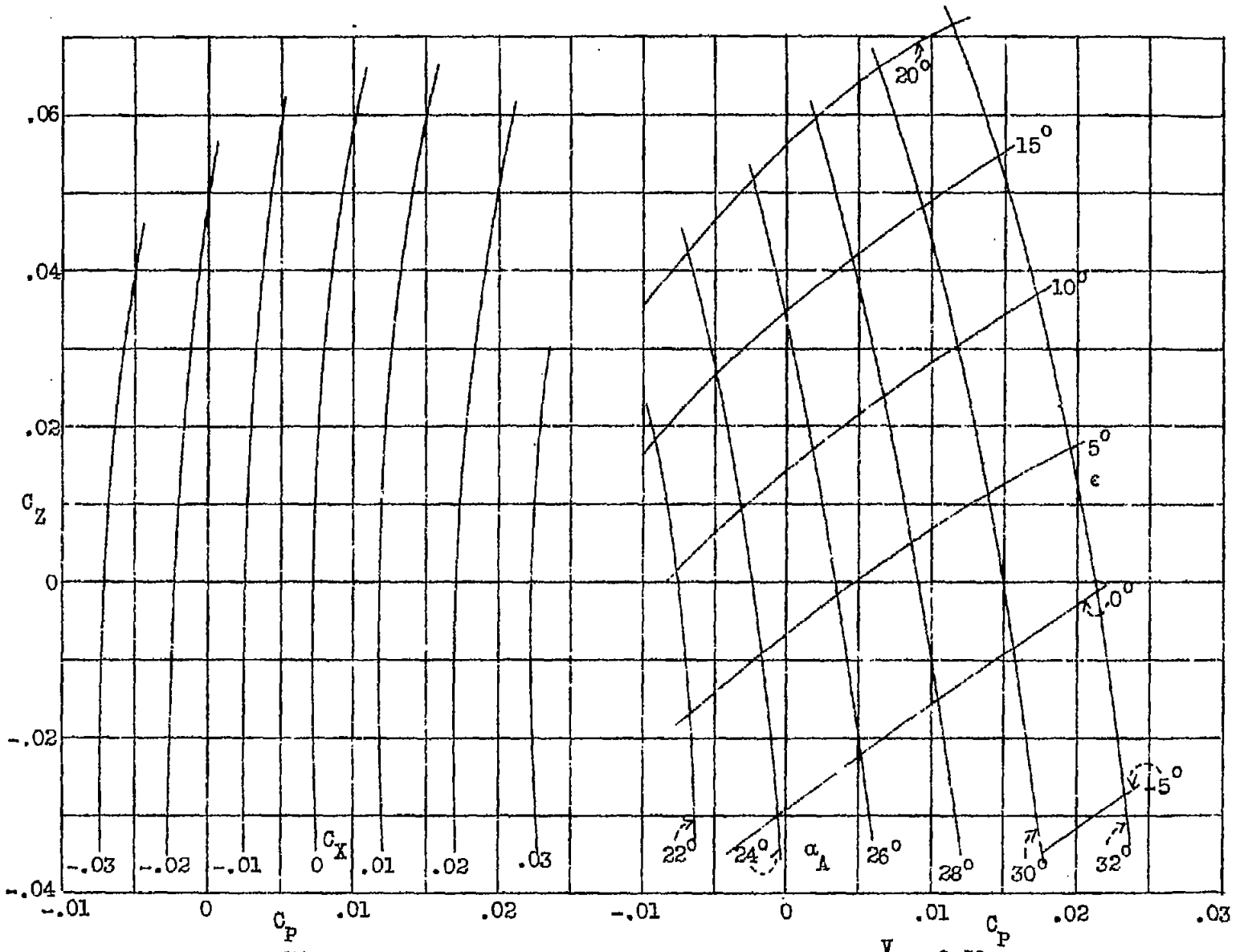

Figure 13.-Level flight. Blades alone; $\Omega R = 150$; $\frac{V}{\Omega R} = 0.50$

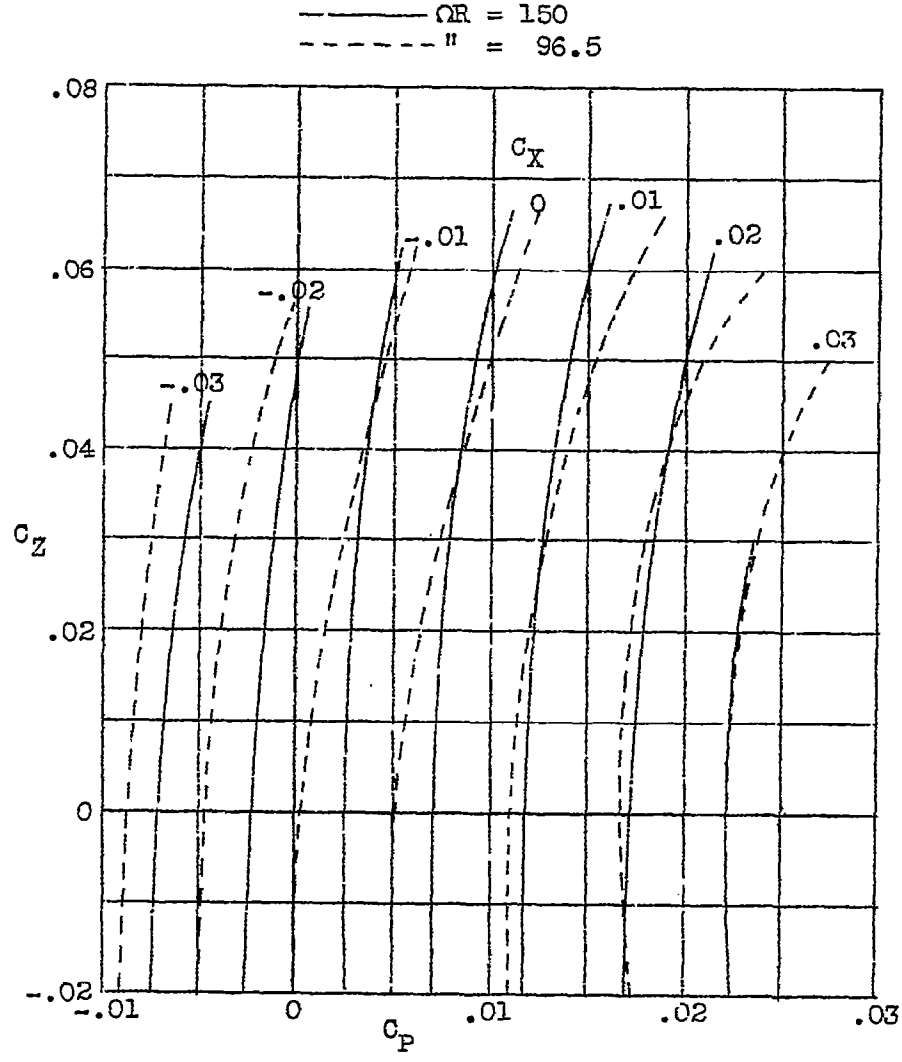

Figure 14.-Scale effect. Level flight. Blades alone; $\frac{V}{\Omega R} = 0.50$

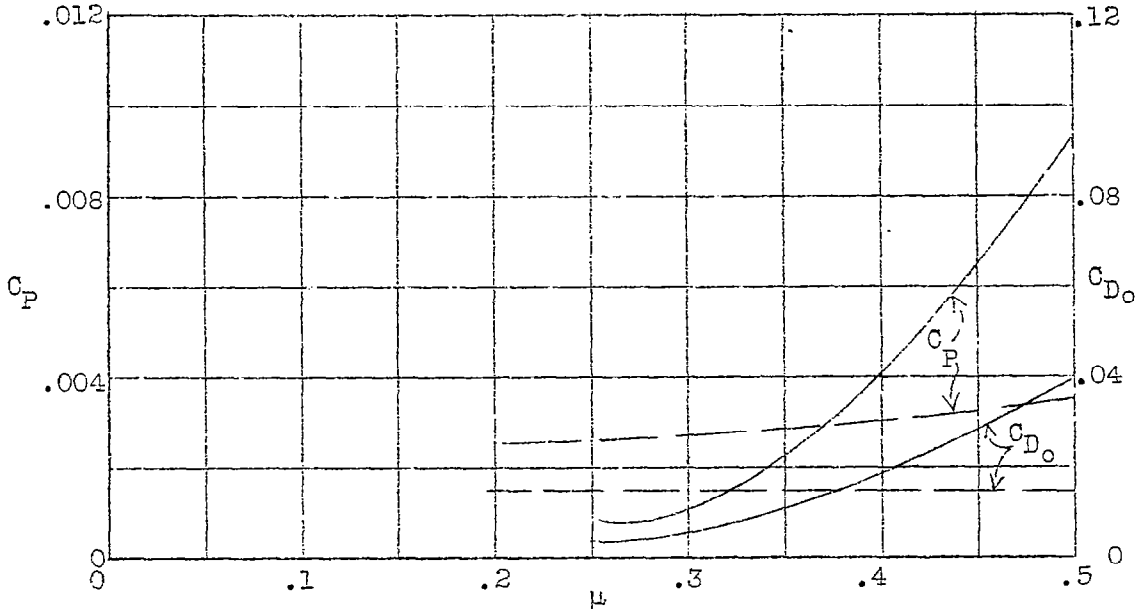

Figure 15.-Comparison of computed and experimental results of C_P and C_{D_o} when C_X and C_Z are zero.

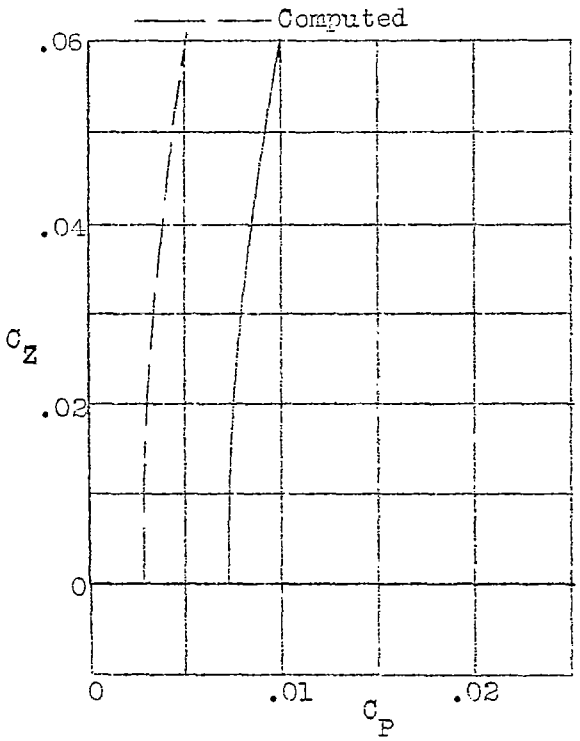

Figure 16.-Comparison of computed and experimental results of $C_P=f(C_Z)$ for $C_X = 0$ and $\mu = 0.50$.

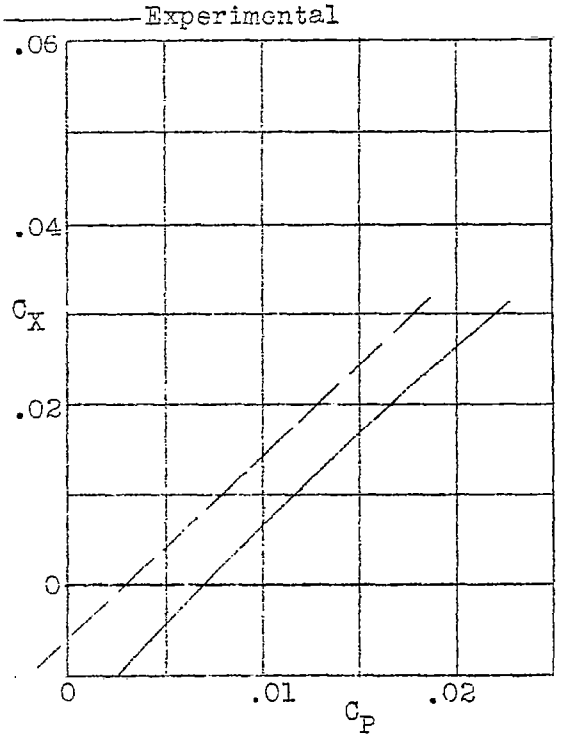

Figure 17.-Comparison of computed and experimental results of $C_P=f(C_X)$ for $C_Z=0$ and $\mu = 0.50$.

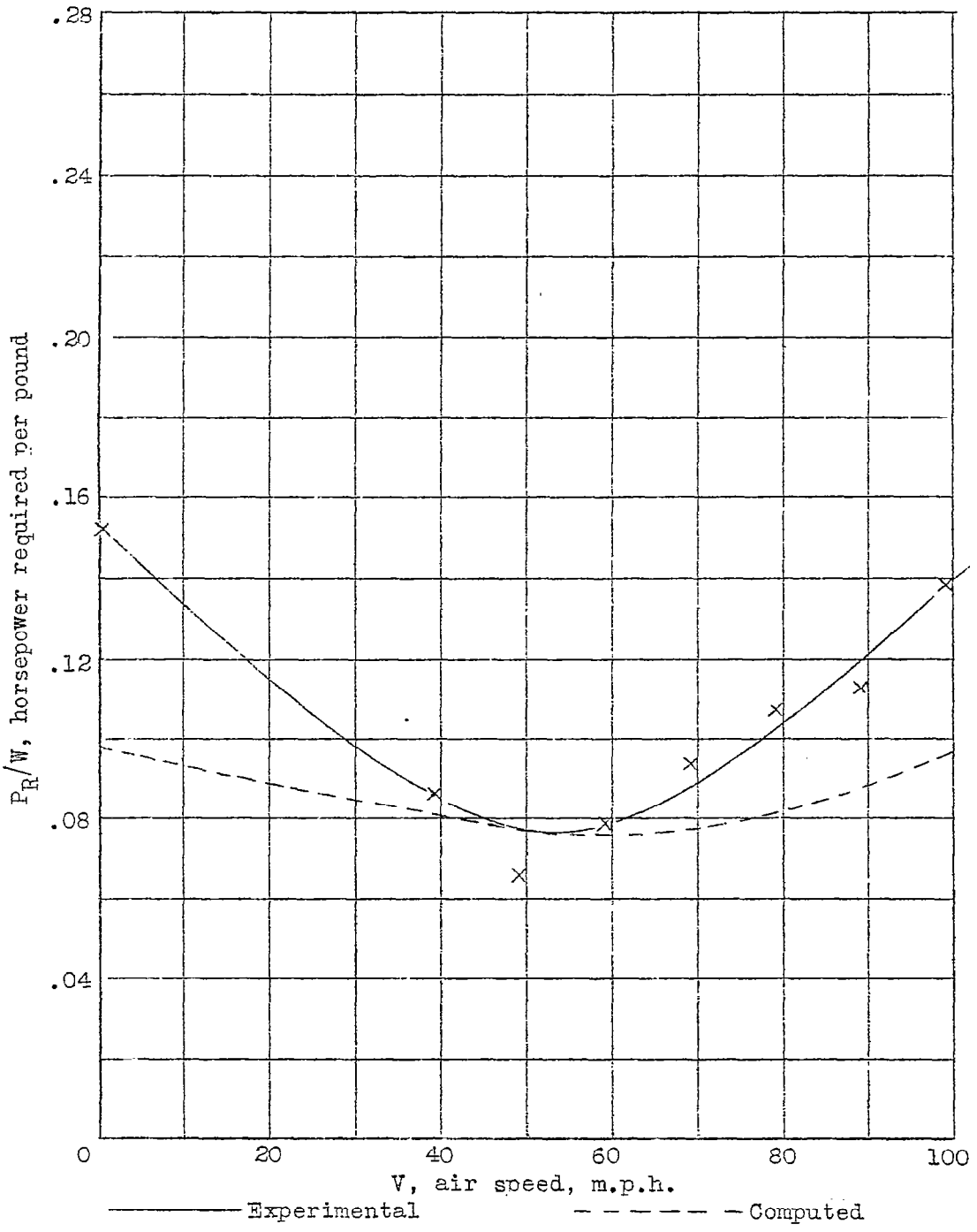

Figure 18.-Cyclogiro performance calculation.

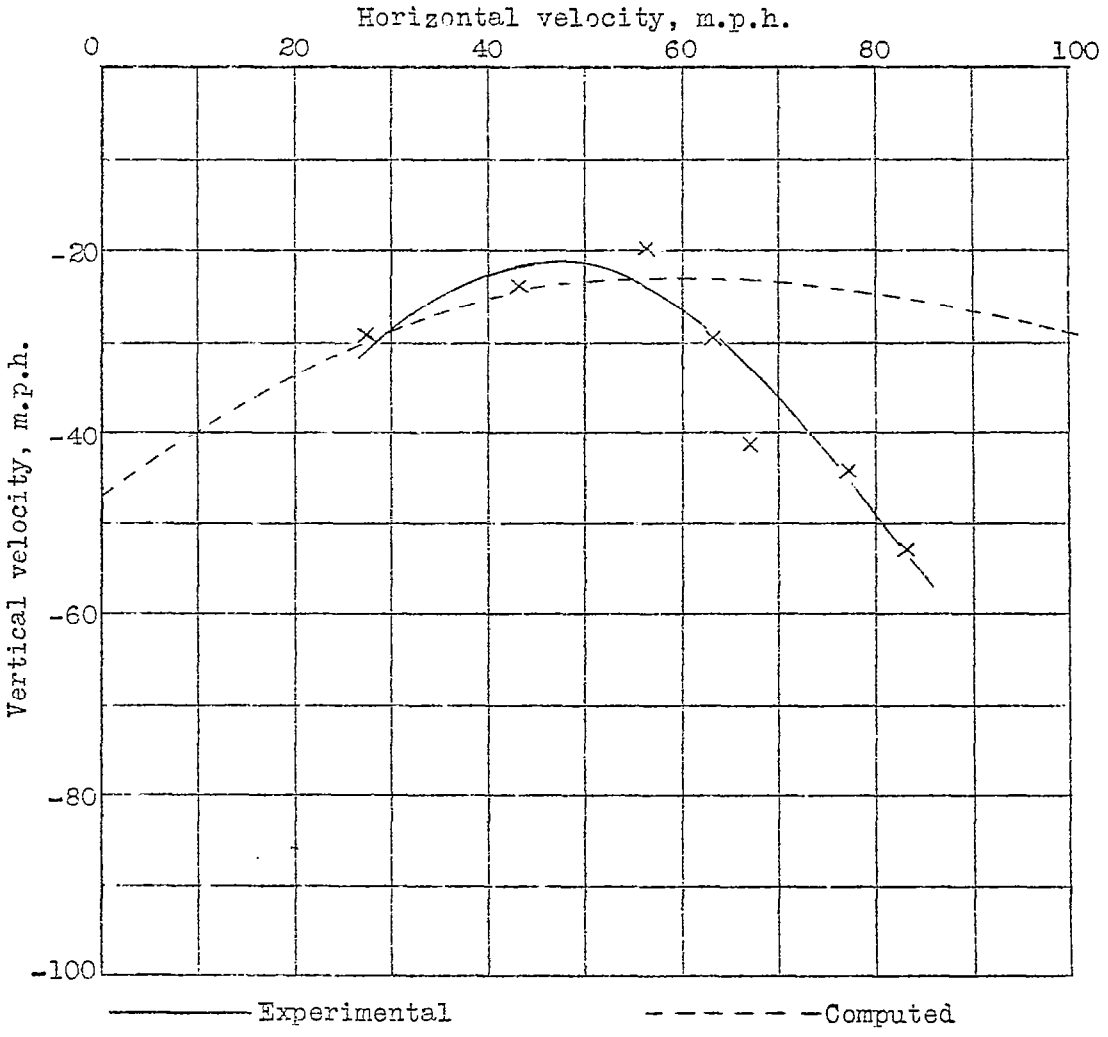

Figure 19.-Autorotation of cyclogiro.